Combined Raman and infrared investigation of the insulator-to-metal transition in $NiS_{2-x}Se_x$ compounds

C. Marini,[1,2] A. Perucchi,[2,3] D. Chermisi,[2] P. Dore,[4] M. Valentini,[2] D. Topwal,[5] D. D. Sarma,[5] S. Lupi,[2] and P. Postorino[2]

[1]*European Synchrotron Radiation Facility, 6 Rue Jules Horowitz, Boîte Postale 220, F-38043 Grenoble Cedex, France*

[2]*CNR-IOM and Dipartimento di Fisica, Università di Roma "La Sapienza", Piazzale Aldo Moro 2, I-00185 Roma, Italy*

[3]*Sincrotrone Trieste S.C.p.A., Area Science Park, I-34012 Basovizza, Trieste, Italy*

[4]*CNR-SPIN and Dipartimento di Fisica, Università di Roma "La Sapienza", Piazzale Aldo Moro 2, I-00185 Roma, Italy*

[5]*Solid State and Structural Chemistry Unit, Indian Institute of Science, Bangalore 560012, India*

(Received 29 September 2011; revised manuscript received 5 December 2011; published 21 December 2011)

Ambient-condition Raman spectra were collected in the strongly correlated $NiS_{1-x}Se_x$ pyrite ($0 \leqslant x \leqslant 1.2$). Two samples ($x = 0$ and $x = 0.55$) were studied as a function of pressure up to 10 GPa, and for the $x = 0.55$ sample the pressure dependence of the infrared reflectivity was also measured (0–10 GPa). This gave a complete picture of the optical response of that system on approaching the metallic state both by application of pressure and/or by Se alloying, which corresponds to a volume expansion. A peculiar nonmonotonic (V-shaped) volume dependence was found for the quasiparticle spectral weight of both pure and Se-doped compounds. In the $x = 0.55$ sample the vibrational frequencies of the chalcogen dimer show an anomalous volume dependence on entering the metallic phase. The abrupt softening observed, particularly significant for the Se-Se pair, indicates the relevant role of the softness of the Se-Se bond as previously suggested by theoretical calculations.

DOI: 10.1103/PhysRevB.84.235134 PACS number(s): 71.30.+h, 62.50.−p, 78.30.Na, 63.20.kd

I. INTRODUCTION

The insulator to metal transition (IMT) in strongly correlated electron systems is a subject of considerable interest in condensed matter research[1–3] mainly because of a number of issues about the underlying driving microscopic mechanisms which need to be addressed. An almost unique opportunity to study from both a theoretical and an experimental point of view the IMT in a narrow-d-band system is offered by the $NiS_{2-x}Se_x$ family, where the transition can be obtained either chemically through the Se substitution in the S site and/or by application of external pressure. The parent compounds of this family, although isoelectronic and isostructural (cubic structure), show completely different electronic properties, with NiS_2 usually referred to as a charge transfer[4] (CT) or covalent[5,6] insulator and $NiSe_2$ as metal.[7,8] At room temperature, indeed, an x-driven IMT occurs for a Se concentration $x \sim 0.6$. The progressive substitution of S by Se enhances the $2p$-band dispersion and increases the d-p hybridization.[1] As a consequence the reduced CT gap (Δ) and the increased electronic bandwidth (W) give rise to the IMT which preserves the cubic crystal structure.[9,10] The T-x phase diagram is shown in Fig. 1. The system exhibits an antiferromagnetic insulator (AFI) ground state for zero and low Se content, it enters an antiferromagnetic metallic (AFM) phase around $x = 0.4$, and a paramagnetic metallic (PM) ground state is finally achieved for $x \geqslant 1$ (see Ref. 11). Following Mott's original idea, application of a hydrostatic pressure P is an alternative way to induce a metallic state.[12] A pressure-induced metallic phase has indeed been achieved in different $NiS_{2-x}Se_x$ systems.[13–15] As the overall cubic structure of the $NiS_{2-x}Se_x$ family does not change in either the pressure-induced or the Se-induced IMT, insulating and metallic states with different microscopic characteristics can thus be achieved within a single structural phase by properly tuning x and P. These structure-independent IMTs, which experimentally realize Mott's original proposition, make the $NiS_{2-x}Se_x$ system particularly suitable for a systematic investigation of electron correlation effects in establishing the metallic state.

Recently, we studied the pressure and the Se-alloying effects in $NiS_{2-x}Se_x$ samples by using infrared (IR) spectroscopy. In particular, we performed reflectance measurements at room temperature (T) on four samples ($x = 0.00$, 0.55, 0.60, and 1.20). Note that, at ambient conditions, the $x = 0.00$ and $x = 0.55$ samples are insulating and the $x = 0.60$ and $x = 1.20$ samples are metallic, as shown in Fig. 1. The reflectance measurements we also performed as a function of pressure on a NiS_2 sample showed a pressure-induced IMT from an insulating to a metallic phase. Our previous results show that, besides similarities between the P- and Se-dependent phase diagrams, the simple linear scaling between P and x suggested by transport measurements[14] does not hold at finite frequencies. In particular, the analysis of the IR data indicated that the x- and the P-driven metallization relates to two distinct microscopic mechanisms. These have been captured by local density approximation (LDA) calculations in terms of the three fundamental parameters for the IMT: the bandwidth W, the Coulomb repulsion (U), and the CT gap Δ. On applying external pressure the W/U ratio increases, triggering the IMT; on the contrary, upon Se alloying W/U decreases whereas increase of the W/Δ ratio is responsible for the x-induced IMT.[10]

Another scenario has been proposed in a very recent paper.[16] Here the bonding-antibonding splitting in the S-S (Se-Se) dimer was found to be the main parameter controlling the size of the charge transfer gap. Furthermore, the pressure sensitivity of the low-energy electrodynamics in the Se-doped compound was found to be larger than in the pure compound. This last result was ascribed to the different strengths of the bond within the chalcogenide dimers.[16]

Although these findings should suggest a careful investigation of the lattice dynamics, scarce attention has been devoted until now to the importance of the lattice degree of

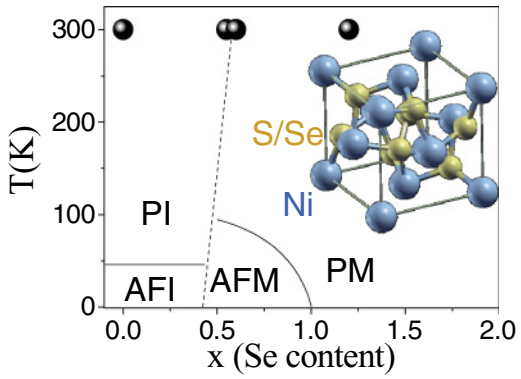

FIG. 1. (Color online) T-x (Se content) phase diagram of $NiS_{2-x}Se_x$ after Ref. 11. Solid symbols indicate the Se content of the investigated samples and working temperature. The pyritic crystal structure is also sketched.

freedom across the IMTs and to the possible role played by charge-lattice couplings.

In the past we showed that the combined use of IR and Raman spectroscopy represents a powerful tool to study the interplay among the different microscopic interactions simultaneously at work in a strongly correlated electron system.[17–20] Indeed, for bad metals also, the IR spectrum is dominated by the response of the charge carriers[1,2,10,21] and can provide direct information on the low-energy electrodynamics, whereas Raman spectra provide information about lattice dynamics and charge-lattice coupling. The combined use of the two techniques can thus be particularly helpful also in the investigation of the charge-delocalization process across the IMT in $NiS_{2-x}Se_x$. Moreover, both Raman scattering and IR spectroscopy can be coupled to the high-pressure technique, allowing a systematic investigation of lattice and electronic response to volume variation.

In the present paper, after the experimental section where the samples and the experimental procedures and equipment are briefly described, we report on ambient-condition Raman measurements on four $NiS_{2-x}Se_x$ samples ($x = 0.00$, 0.55, 0.60, and 1.20; see Fig. 1). The effects of applied pressure on the Raman spectra of the $x = 0.00$ and $x = 0.55$ samples and on the IR spectrum of the $x = 0.55$ sample are then described and discussed in detail. The present findings together with our previous results[10] on the P dependence of the IR spectrum of NiS_2 allow a deeper insight into the P and x dependence of the low-energy electrodynamics and lattice dynamics in the $NiS_{2-x}Se_x$ system.

II. EXPERIMENT

High-quality polycrystalline samples of $NiS_{2-x}Se_x$ were grown by reacting pure elements in stoichiometric ratios, with 5%–10% of the chalcogens taken in excess, in order to compensate for evaporation. The elements were sealed in evacuated (10^{-5} torr) quartz ampules, and heated to 450 K for a week. Samples were fully characterized by x-ray diffraction, resistivity, and photoemission measurements.[22]

A screw-clamped opposing-plates diamond anvil cell (DAC) equipped with 400 μm culet II A diamonds has been used for both Raman and IR high-pressure experiments. The gaskets were made of a 250-μm-thick steel foil with a sample chamber of 130 μm diameter and 40 to 50 μm height under working conditions. We used NaCl as P-transmitting medium for both Raman and IR measurements. Pressure was measured *in situ* with the standard ruby fluorescence technique.[23]

Raman measurements were carried out by means of a confocal-microscope Raman spectrometer, equipped with 50× and 20× long working distance objectives, a 16 mW He-Ne laser (632.8 nm wavelength), and an 1800 lines/mm grating monochromator with a charge-coupled device detector. Raman spectra were collected in the backscattering geometry and a notch filter was used to reject the elastic contribution. Under these experimental conditions we achieved a few-micrometer -diameter laser spot on the sample and a spectral resolution better than 3 cm^{-1}.

High-P IR reflectivity spectra of samples in the DAC were collected at room temperature by exploiting the high brilliance of the SISSI infrared beamline at the ELETTRA synchrotron.[24] The incident and reflected radiation were focused and collected by a cassegrain-based Hyperion 2000 infrared microscope equipped with both MCT and bolometer detectors and coupled to a Bruker IFS 66v interferometer, which allows exploration of the 250–10 000 cm^{-1} spectral range.

III. RAMAN SPECTRA UNDER AMBIENT CONDITIONS

Raman spectra of the four $NiS_{2-x}Se_x$ compounds were collected up to 1100 cm^{-1}. They are shown in Fig. 2 over the

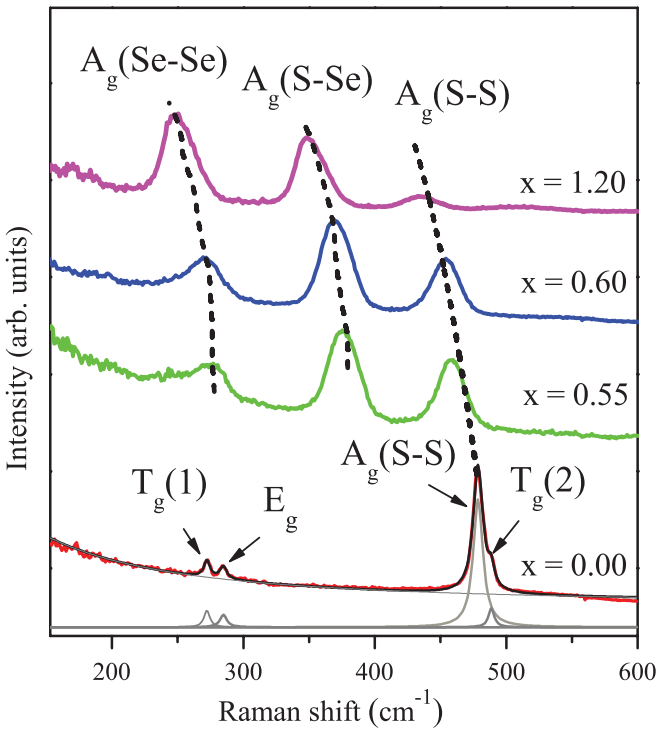

FIG. 2. (Color online) Raman spectra at ambient conditions of $NiS_{2-x}Se_x$ compounds. Best fit profile (black curve) is reported for the $x = 0.00$ sample. DHO phonon contributions and electronic contributions (gray lines) are also reported.

150–600 cm^{-1} range since no detectable spectral features were observed above 550 cm^{-1}. These spectra are in qualitative agreement with literature data.[9,26] According to the factor group analysis (space group T_h^6), five Raman-active modes $A_g + E_g + 3T_g$ are expected. Since Ni atoms are at a center of inversion, all the Raman modes involve only displacements of the chalcogen atoms X (X = S or Se). Raman spectroscopy is thus intrinsically particularly sensible to the S-Se chemical substitution.

The NiS_2 spectrum shown in Fig. 2 consists of only four out of the five expected phonon peaks: two very weak peaks around 270 cm^{-1} and two peaks at ~470 cm^{-1} (i.e., one intense peak and a shoulder on its high-frequency side). According to Ref. 9, the low-frequency doublet is ascribed to the pair librations [$T_g(1)$ and E_g modes], and the high-frequency doublet to in-phase and out-of-phase stretching vibrations of the S-S pairs[9,26] [i.e., the most intense peak to the A_g mode and the shoulder to the $T_g(2)$]. It is worth noting that none of the previous Raman data reported in the literature show all the five predicted peaks as the $T_g(3)$ mode is always missing.[9,26,28]

The chemical substitution of S by Se activates in principle new modes involving all the possible X-X pairs. For a given symmetry the peaks ascribed to the Se-Se, Se-S, and S-S pairs are expected at increasing frequencies since the reduced mass of the pairs decreases going from Se-Se to Se-S to S-S. On these bases and following the assignment reported in Ref. 9, we can ascribe the three main peaks in the spectra of the Se-doped compounds to Se-Se, Se-S, and S-S pairs, going from low to high frequency (see Fig. 2). The frequencies observed for the three peaks are indeed in a rather good agreement with a scaling based on the square root of the chalcogen pair reduced masses. In particular, considering that the A_g mode in the parent compounds is by far the most intense peak (see Fig. 2 for NiS_2 and Ref. 9 for $NiSe_2$), the three peaks which characterize the spectra at intermediate doping can be mainly ascribed to the A_g mode. This assignment is also qualitatively confirmed by looking at the x dependence of the peak intensities in Fig. 2. Indeed, as expected, on increasing the Se content the intensity of the A_g(Se-Se) mode is enhanced, whereas that of the A_g(S-S) mode is depressed. The intensity of the A_g(Se-S) mode is enhanced up to $x = 0.6$ and depressed on further increase in the Se content above $x = 1$, compatibly with a random substitution model. Finally, the very small peaks detectable at ~175 cm^{-1} in the spectrum of the sample with the highest Se content ($x = 1.2$) can be ascribed to the low-frequency librations of the Se-Se pairs. We notice additionally that the extent of disorder induced by S-Se chemical substitution also has a broadening effect on the phonon peaks. It is finally important to point out that the generalized softening of the peak frequencies must be ascribed to the volume expansion occurring on increasing the Se content.[9]

Measured spectra were fitted by using a standard model curve[20,25] given by the sum of an electronic component plus phonon contributions, each described by a damped harmonic oscillator (DHO). Good fits of all the Raman spectra were obtained, as shown in Fig. 2 for the $x = 0.00$ spectrum. A detailed analysis of the fitting procedures and results will be reported in a forthcoming paper.

IV. RAMAN SPECTRA UNDER PRESSURE

Raman spectra of the $x = 0.00$ and $x = 0.55$ compounds loaded in the DAC have been collected at different pressures. The fitting procedure introduced above allowed a good description of all the measured spectra by using the same number of phonon components considered at ambient conditions and by subtracting a linear baseline plus the diamond contribution to account for the background signal.[20] The background-subtracted spectra of NiS_2 and of $NiS_{1.45}Se_{0.55}$ collected at different pressures are shown in Fig. 3.

In the NiS_2 case, the progressive lattice compression causes at first a clear hardening of the phonon peak frequencies and the merging of low-frequency $T_g(1)$ and E_g lines into a single band. In the higher-pressure regime, the phonon frequencies only slightly increase and, for $P > 3.8$ GPa the S-S stretching mode apparently splits into two components around 470 cm^{-1} ($p470$) and 480 cm^{-1} ($p480$). A fifth DHO component was then introduced in the fitting procedure. The resulting pressure dependence of the phonon frequencies is shown in Fig. 4. It is unlikely that the origin of this doublet could be ascribed to strongly nonhydrostatic conditions since the absence of a remarkable P gradient has been verified by comparing the spectra collected from different points over the sample surface. Moreover, recent high-P Raman measurements on the similar FeS_2 pyrite have proved that nonhydrostaticity mainly affects the widths of phonons, without significantly modifying their peak frequencies and the P dependence of their intensities.[29] The doublet might be due to the appearance of the missing $T_g(3)$ mode (in Ref. 27 ascribed to a combination of librational and stretching phonon modes), masked at ambient P by the intense A_g mode. Unfortunately it is rather difficult to give a reliable assignment of the $p470$ and $p480$ peaks. On one side we can argue that the pressure-induced hardening of the A_g frequency removes the accidental degeneracy and allows observation of the $T_g(3)$ peak, less sensitive to lattice compression, emerging from the low-frequency tail of the

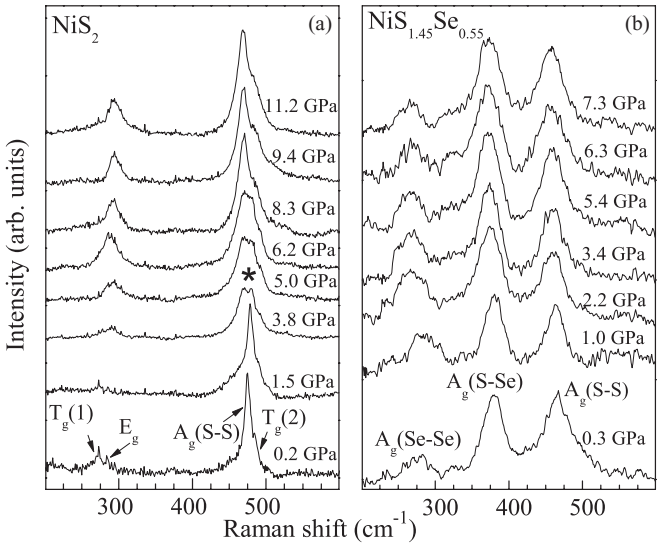

FIG. 3. Background-subtracted Raman spectra of the $x = 0.00$ (a) and $x = 0.55$ (b) $NiS_{2-x}Se_x$ samples as a function of pressure. The star on the spectrum collected at $P = 3.8$ GPa marks the appearance of the $p470$-$p480$ doublet (see text).

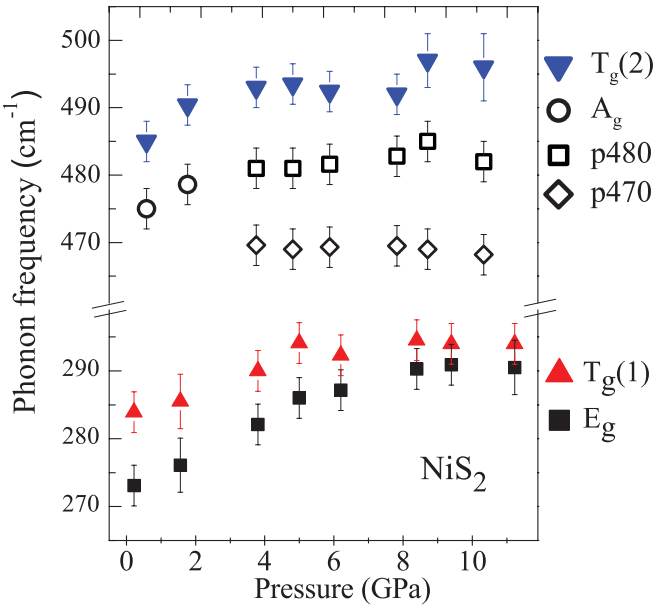

FIG. 4. (Color online) Pressure dependence of the phonon frequencies of NiS_2.

A_g peak. On the other side we can conjecture an abrupt softening of the A_g peak that unveils the $T_g(3)$, which remains at frequency higher than that of the A_g peak. Although the latter choice might be preferred on the basis of the pressure dependence of the peak intensities, a definite conclusion on the assignment of the doublet components [$p470 \rightarrow T_g(3)$ and $p480 \rightarrow A_g$ or vice versa] cannot be drawn.

In the $x = 0.55$ sample, high P does not affect the three-mode structure observed at ambient conditions. Results provided by the fitting procedure are shown in Fig. 5. Here, at

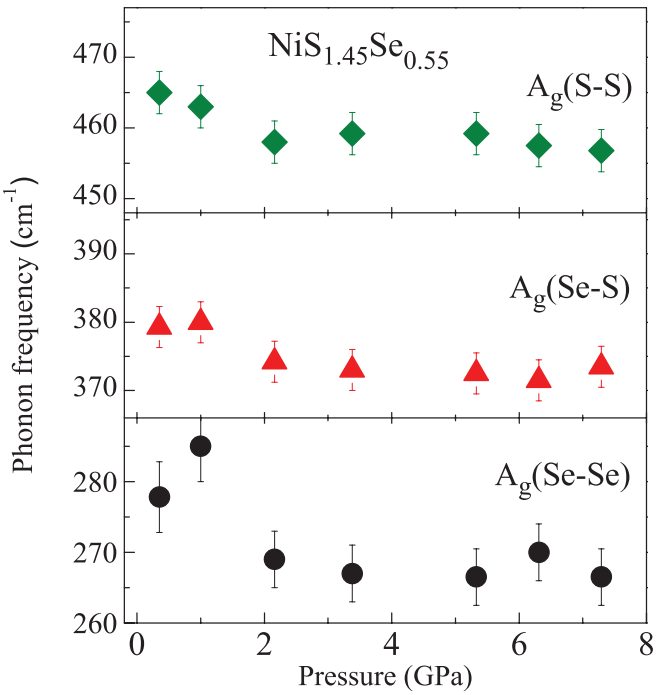

FIG. 5. (Color online) Pressure dependence of the phonon frequencies of $NiS_{1.45}Se_{0.55}$.

variance with the NiS_2 case, a general softening for all modes can be observed as a function of P. In particular an anomalous and abrupt softening of the phonon frequencies is indeed clear for all the phonon frequencies above 1 GPa, although this effect is much more pronounced for the Se-Se mode than for the S-Se and S-S modes.

V. PRESSURE-DEPENDENT IR MEASUREMENTS

Infrared reflectivity $R(\omega)$ spectra of the $NiS_{1.45}Se_{0.55}$ sample have been collected as a function of pressure. We used experimental and analysis procedures equivalent to those employed for the previous measurements on NiS_2.[10] The $R(\omega)$ spectra measured by using the DAC at the diamond-sample interface are reported in Fig. 6 for pressures between 1.3 and 6.3 GPa and from the far to the near IR (250–10 000 cm^{-1}). The zero-pressure reflectance spectrum, as previously evaluated at the diamond-sample interface,[10] is also shown for comparison. Note that the multiphonon diamond absorption prevents the collection of reliable data in the 1600–2300 cm^{-1} range. With increasing pressure, $R(\omega)$ is progressively enhanced at low energy, as already observed in the NiS_2 case.[10]

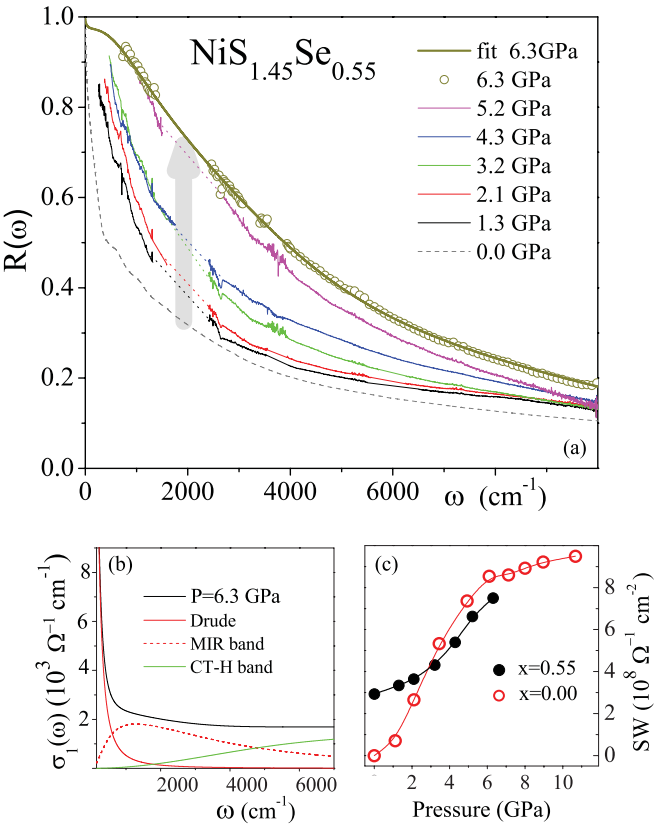

FIG. 6. (Color online) (a) $R(\omega)$ measured at the sample-diamond interface at high pressures, and evaluated at ambient pressure (dashed line), from Ref. 10. The best-fit curve of the 6.3 GPa spectrum is also reported (bold line). (b) Optical conductivity $\sigma_1(\omega)$ and its components from the best fit of the 6.3 GPa spectrum. (c) Quasiparticle spectral weight SW as a function of P for $x = 0.55$ and for $x = 0.00$ from Ref. 10.

The optical conductivity $\sigma_1(\omega)$ was obtained by using standard procedures to describe the $R(\omega)$ spectrum based on the Drude-Lorentz model.[30,31] As in the case of our previous IR measurements,[10] good descriptions of $R(\omega)$ and, correspondingly, of $\sigma_1(\omega)$ can be obtained by using a Drude term, a broad mid-infrared contribution centered around 2000 cm^{-1}, and an intense high-frequency oscillator centered around 10 000 cm^{-1} which mimics the CT and Hubbard transitions (CT-H band).[10] As an example, the best-fit curve of the 6.3 GPa spectrum and its components is reported in Fig. 6(a), the corresponding $\sigma_1(\omega)$ in Fig. 6(b). As discussed in the past,[10,21,32] the Drude component can be attributed to the quasiparticle (QP) coherent excitations around the Fermi energy; the mid-IR component to QP transitions from the QP peak to the upper and lower Hubbard bands. The quasiparticle spectral weight (SW), defined as the integrated area of Drude plus mid-IR components, is reported as a function of pressure in Fig. 6(c). For comparison, the SW previously obtained for NiS_2 at different pressures[10] is reported in the same figure. In this case the SW is nearly zero at ambient P and then increases owing to gradual transformation from the insulating to the metallic state, when correlation effects get smaller as a consequence of the Mott transition.[10] In the $x = 0.55$ case, the SW is already finite at zero pressure because of free charges due to the presence of the Se atoms. This explains why the Raman response is weaker in the $x = 0.55$ case with respect to the $x = 0.00$ case. With increasing pressure, the SW increases and a change of the slope is observed above ~2 GPa, although a clear and unambiguous signature of the crossover to a metallic phase cannot be found.

VI. DISCUSSION AND CONCLUSIONS

The measurements here presented together with those reported in Ref. 10 provide data on the pressure and the Se-alloying dependence of both the phonon frequencies (Raman) and the quasiparticle spectral weight (IR) of the $NiS_{2-x}Se_x$ system. Bearing in mind that on applying pressure the volume is compressed while it is expanded on increasing x, all the data can be plotted together by considering their dependence on the volume. For the volume expansion (Se alloying), x-ray diffraction data are available in the literature,[9] while for the volume compression (P) structural data[33] are available for NiS_2 only up to 6.5 GPa. A reliable estimate of the volume P dependence for the $x = 0.55$ compound can however be obtained by applying the procedure used for NiS_2 in Ref. 10. We point out that this procedure has given volume values for NiS_2 in very good agreement with the available experimental data[33] and with those resulting from LDA calculations up to at least 10 GPa (see Ref. 10). Both the spectral weights (present data and Ref. 10) and the stretching frequencies of all the chalcogen pairs (S-S, S-Se, Se-Se) can thus be plotted as functions of the volume in Fig. 7.

In Fig. 7(a) the volume dependence of the SWs is drawn. The data for NiS_2 from Ref. 10 show a clear nonmonotonic (V-shaped) behavior with a minimum occurring at $V^0_{x=0} = 183.6$ A^3, which is the volume of the unit cell at ambient conditions. The present data on $NiS_{1.45}Se_{0.55}$ show a similar V-shaped behavior, although remarkably less pronounced and with the minimum at $V^0_{x=0.55} = 191.5$ A^3. The volume dependence for the S-S, S-Se, and Se-Se stretching frequencies shown in Figs. 7(b), 7(c), and 7(d) are rather similar, at least within the high- and the low-volume regions. Indeed, at low volume, all the frequencies appear to be actually volume independent whereas, on the high-volume side for $V \geqslant 188$ A^3, a clear frequency softening occurs on volume expansion.

Within the intermediate-volume region, an anomaly in a narrow volume region around 186 A^3 (see the hatched stripe in Figs. 7(b), 7(c), and 7(d)) occurs in the volume dependence of the three stretching frequencies in the case of the $x = 0.55$ sample. Note that this anomaly becomes more and more remarkable on going from S-S to S-Se to Se-Se. For the sake of comparison, a second hatched stripe is drawn in Figs. 7(a) and 7(b) at around 178 A^3, which corresponds to an applied pressure on the pure sample over the 2.5–3.5 GPa range [see the pronounced sigmoidal behavior of the SW shown in Fig. 6(c)]. In the NiS_2 case, if $p480$ is associated with the A_g(S-S) mode no discontinuity in the S-S stretching

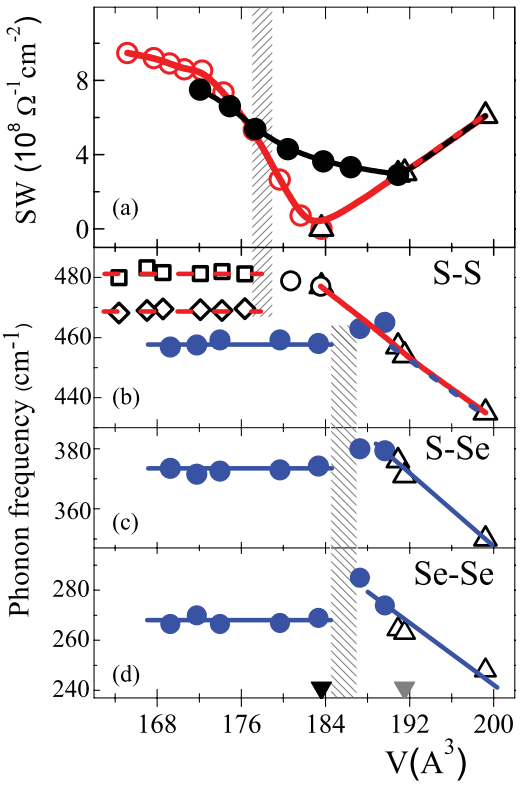

FIG. 7. (Color online) (a) Quasiparticle spectral weight of $NiS_{2-x}Se_x$ as a function of volume: open circles, $x = 0.00$ (Ref. 10); full circles, $x = 0.55$ (present data); triangles, ambient conditions, $x = 0.00$, 0.55, 0.60, and 1.20 (Ref. 10). Volume dependencies of the A_g stretching frequencies of the S-S (b), Se-S (c), and Se-Se (d) dimers for $x = 0.00$ (open circles), $x = 0.55$ samples (full circles), and ambient-condition $x = 0.00$, 0.55, 0.60, and 1.20 samples (triangles). Open diamonds and squares in (b) refer to the $p470$ and $p480$ peaks, respectively. The hatched stripe crossing (a) and (b) marks the volume region around 178 A^3; the stripe crossing (b), (c), and (d) marks the volume region around 186 A^3 (see text). Black and gray down triangles on the V axis point out the volume values at ambient conditions for $x = 0.00$ and $x = 0.55$ samples. In all the panels full lines are guides to the eye.

frequency occurs. On the contrary, if $p470$ corresponds to the A_g(S-S) mode, a discontinuity becomes evident. The anomalies in the V dependence of phonons indicate that the crossover from insulating to metallic phase affects the lattice dynamics in the $x = 0.55$ Se-doped sample, while the present data do not allow us to draw a definite conclusion in the NiS_2 case.

In conclusion, in Se-doped samples the metallization process influences significantly the phonon spectrum, and the charge-lattice coupling may play a relevant role in the IMT. Moreover, it is rather clear that Se atoms play a key role in the charge-delocalization process of doped compounds. Furthermore, the pressure-induced band gap closure[16] appears to be correlated both with the rigidity of the S-S dimer, which shows a bond length nearly constant under compression, and with the softness of the Se-Se dimer, which, on the contrary, shows a bond length expansion. It is worth noting that in Se-doped samples the anomaly in the stretching frequencies clearly increases on going from S-S to S-Se and to Se-Se, thus confirming the relevant role of the softness of the Se-Se dimer in the case of the doped compounds.[16] Although theoretical results previously reported are fully consistent with the present experimental findings, our high-pressure Raman results and in particular the anomalous behavior of the stretching mode volume dependence around the metallization transition demand a further theoretical and experimental effort to determine in a clear way the role played by the lattice dynamics in the transition.

[1] H. Imada, A. Fujimori, and Y. Tokura, Rev. Mod. Phys. **70**, 1039 (1998).

[2] S. Lupi, L. Baldassarre, B. Mansart, A. Perucchi, A. Barinov, P. Dudin, E. Papalazarou, F. Rodolakis, J.-P. Rueff, J.-P. Itié, S. Ravy, D. Nicoletti, P. Postorino, P. Hansmann, N. Parragh, A. Toschi, T. Saha-Dasgupta, O. K. Andersen, G. Sangiovanni, K. Held, and M. Marsi, Nat. Commun. **1**, 105 (2010).

[3] L. Baldassarre, A. Perucchi, S. Lupi, and P. Dore, J. Phys.: Condens. Matter **22**, 355402 (2010).

[4] J. Zaanen, G. A. Sawatzky, and J. W. Allen, Phys. Rev. Lett. **55**, 418 (1985).

[5] S. R. Krishnakumar and D. D. Sarma, Phys. Rev. B **68**, 155110 (2003).

[6] D. D. Sarma, S. R. Krishnakumar, E. Weschke, C. Schüßler-Langeheine, Chandan Mazumdar, L. Kilian, G. Kaindl, K. Mamiya, S.-I. Fujimori, A. Fujimori, and T. Miyadai, Phys. Rev. B **67**, 155112 (2003).

[7] X. Yao, J. M. Honig, T. Hogan, C. Kannewurf, and J. Spalek, Phys. Rev. B **54**, 17469 (1996).

[8] J. M. Honig and J. Spalek, Chem. Mater. B **10**, 2910 (1998).

[9] C. de las Heras and F. Agull-Rueda, J. Phys.: Condens. Matter **12**, 5317 (2000).

[10] A. Perucchi, C. Marini, M. Valentini, P. Postorino, R. Sopracase, P. Dore, P. Hansmann, O. Jepsen, G. Sangiovanni, A. Toschi, K. Held, D. Topwal, D. D. Sarma, and S. Lupi, Phys. Rev. B **80**, 073101 (2009).

[11] K. Iwaya, Y. Kohsaka, S. Satow, T. Hanaguri, S. Miyasaka, and H. Takagi, Phys. Rev. B **70**, 161103(R) (2004).

[12] N. F. Mott, Proc. Phys. Soc., London, Sect. A **64**, 416 (1949).

[13] N. Mori and H. Takahashi, J. Magn. Magn. Mater **31**, 335 (1983).

[14] S. Miyasaka, H. Takagi, Y. Sekine, H. Takahashi, N. Mori, and R. J. Cava, J. Phys. Soc. Jpn. **69**, 3166 (2000).

[15] P. G. Niklowitz, P. L. Alireza, M. J. Steiner, G. G. Lonzarich, D. Braithwaite, G. Knebel, J. Flouquet, and J. A. Wilson, Phys. Rev. B **77**, 115135 (2008).

[16] J. Kunes, L. Baldassarre, B. Schächner, K. Rabia, C. A. Kuntscher, Dm. M. Korotin, V. I. Anisimov, J. A. McLeod, E. Z. Kurmaev, and A. Moewes, Phys. Rev. B **81**, 035122 (2010).

[17] P. Postorino, A. Congeduti, E. Degiorgi, J. P. Itie, and P. Munsch, Phys. Rev. B **65**, 224102 (2002)

[18] A. Sacchetti, M. Cestelli Guidi, E. Arcangeletti, A. Nucara, P. Calvani, M. Piccinini, A. Marcelli, and P. Postorino, Phys. Rev. Lett. **96**, 035503 (2006).

[19] E. Arcangeletti, L. Baldassarre, D. Di Castro, S. Lupi, L. Malavasi, C. Marini, A. Perucchi, and P. Postorino, Phys. Rev. Lett. **98**, 196406 (2007).

[20] C. Marini, E. Arcangeletti, D. Di Castro, L. Baldassare, A. Perucchi, S. Lupi, L. Malavasi, L. Boeri, E. Pomjakushina, K. Conder, and P. Postorino, Phys. Rev. B **77**, 235111 (2008).

[21] L. Baldassarre, A. Perucchi, D. Nicoletti, A. Toschi, G. Sangiovanni, K. Held, M. Capone, M. Ortolani, L. Malavasi, M. Marsi, P. Metcalf, P. Postorino, and S. Lupi, Phys. Rev. B **77**, 113107 (2008).

[22] D. D. Sarma, M. Pedio, M. Capozi, A. Girycki, N. Chandrasekharan, N. Shanthi, S. R. Krishnakumar, C. Ottaviani, C. Quaresima, and P. Perfetti, Phys. Rev. B **57**, 6984 (1998).

[23] H. K. Mao, P. M. Bell, J. W. Shaner, and D. J. Steinberg, J. Appl. Phys. **49**, 3276 (1978).

[24] S. Lupi, A. Nucara, A. Perucchi, P. Calvani, M. Ortolani, L. Quaroni, and M. Kiskinova, J. Opt. Soc. Am. B **24**, 959 (2007).

[25] S. Yoon, H. L. Liu, G. Schollerer, S. L. Cooper, P. D. Han, D. A. Payne, S. W. Cheong, and Z. Fisk, Phys. Rev. B **58**, 2795 (1998).

[26] V. Lemos, G. M. Gualberto, J. B. Salzberg, and F. Cerdeira, Phys. Status Solidi B **100**, 755 (1980).

[27] C. Sourisseau, R. Cavagnat, and M. Fouassier, J. Phys. Chem. Solids **52**, 537 (1991).

[28] T. Suzuki, K. Uchinokura, T. Sekine, and E. Matsuura, Solid State Commun. **23**, 847 (1977).

[29] A. K. Kleppe and A. P. Jephcoat, Min. Mag. **68**, 433 (2004).

[30] F. Wooten, *Optical Properties of Solids* (Academic Press, New York, 1972).

[31] M. Dressel and G. Grüner, *Electrodynamics of Solids* (Cambridge University Press, Cambridge, 2002).

[32] M. J. Rozenberg, G. Kotliar, H. Kajueter, G. A. Thomas, D. H. Rapkine, J. M. Honig, and P. Metcalf, Phys. Rev. Lett. **75**, 105 (1995).

[33] T. Fujii, K. Tanaka, F. Marumo, and Y. Noda, Miner. J. **13**, 448 (1987).